Mathematical Model for the Ascent and Descent of a High-Altitude Tethered Balloon

GEORGE R. DOYLE JR.*
Goodyear Aerospace Corporation, Akron, Ohio

The ascent and descent dynamics of a balloon-tether system have been studied to determine the feasibility of deploying and retrieving high-altitude tethered balloons through the intermediate-altitude regions of high wind velocity. The development of the computer program for the study is discussed and study results are presented. The derivation of the differential equations of motion and the determination of forces acting on the balloon-tether system are discussed in some detail. Graphs present the effects of wind profile, winching rate, and buoyant lift on balloon launch and retrieval trajectories, cable tension, and dynamic pressure acting on the balloon. The study indicates that a high-altitude balloon-tether system can be launched and retrieved under certain conditions and establishes some preliminary design criteria for balloon, tether, and winch.

Nomenclature

B = buoyant force of the displaced air minus the sum of the vertical drag force and the weights of the lifting gas and the balloon
$D_{H_{ci}}$ = horizontal component of drag on ith cable link
$D_{V_{ci}}$ = vertical component of drag on ith cable link
$\mathbf{e}_i, \mathbf{e'}_i$ = unit vectors describing cable dynamics
$\mathbf{e}_{N+1}, \mathbf{e'}_{N+1}$ = unit vectors describing balloon dynamics
$F_{H_{r-1}}$ = horizontal force acting at the bottom of the rth link ($r = 1, N$)
$\mathbf{F}_i$ = applied force acting on the ith link
$\mathbf{F}_{N+1}$ = applied force acting on harness
$\mathbf{F}_Q$ = applied force acting on balloon
$F_{V_{r-1}}$ = vertical force acting at bottom of rth link ($r = 1, N$)
F_θ = generalized force acting on balloon
$F_{\phi r}$ = generalized force acting on rth cable link ($r = 1, N$)
FS = factor of safety
H = horizontal drag on balloon
I_B = mass moment of inertia of balloon about Q
l_{ci} = length of ith cable link
l_h = length of harness
M = applied moment about the center of mass of the balloon
M_1 = directional mass normal to longitudinal axis of balloon
M_2 = directional mass along longitudinal axis of balloon
m_{ci} = mass of ith cable link
m_h = mass of harness
N = number of cable links
$\mathbf{N}_1, \mathbf{N}_2$ = unit vectors for inertia coordinate system
P_i = top point of ith cable link
P_i^* = center of mass of ith cable link
Q = center of mass of balloon
q_B = dynamic pressure acting on the balloon
SI = Summer I wind profile
T = total kinetic energy of the system
T_b = kinetic energy of balloon and harness
T_c = kinetic energy of cable
T_{r-1} = cable tension at the bottom of the rth link
t = time
V_g = horizontal wind velocity
$\mathbf{V}^{P_n}$ = velocity of P_n
$\mathbf{V}^{P_n*}$ = velocity of P_n^*
$\mathbf{V}^Q$ = velocity of balloon
$\dot{X}$ = horizontal velocity of the balloon
$\dot{Z}$ = vertical velocity of balloon
θ = angular displacement of balloon's longitudinal axis
ϕ_r = angular displacement of rth cable link ($r = 1, N$)

Presented as Paper 68-942 at the AIAA 2nd Aerodynamic Deceleration Systems Conference, El Centro, Calif., September 23–25, 1968; submitted November 18, 1968; revision received May 12, 1969. This study was conducted at Goodyear Aerospace Corporation under contract with the Air Force Cambridge Research Laboratory.

* Development Engineer. Flight Dynamics Department.

Introduction

THE desire to place a payload at an altitude of 100,000 ft and to retrieve it prompted a study of the ascent and descent dynamics of a balloon-tether system. Techniques to analyze such a system were established and a computer program was developed which defines the dynamics of the tether and balloon by integrating the equations of motion.

Figure 1 compares a typical balloon-tether profile with a geometric representation of the system. The actual system might be composed of a naturally shaped tandem balloon supporting a tapered cable.[1] The mathematical model for the study consists of a spherical balloon and a cable made up of N links. The angles ϕ_i (see Fig. 1B) define the cable profile exactly.

Previously, a mathematical model of the motion of a tethered balloon when disturbed from its equilibrium position by a wind gust was constructed and programed on a digital computer.[2] This study extends the mathematical model to include a tether that will increase (or decrease) in length and mass as a function of the winching rate. The number of links to be used by the extended mathematical model and the effects of parameters acting on the system during launch and retrieval are determined in the study.

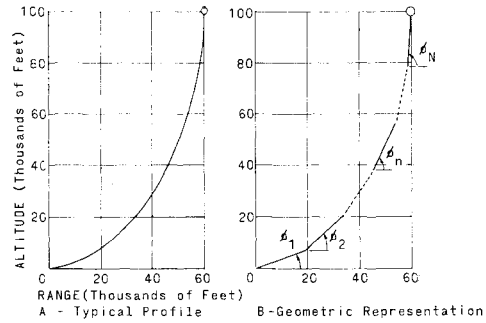

Fig. 1 Balloon-tether system.

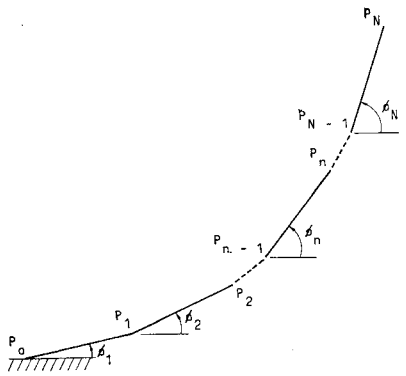

Fig. 2 Tether model.

Equations of Motion

General

The differential equations of motion are derived with the use of Lagrangian techniques and with the assumption that the system can be simulated by a tether of N straight links with the top link hinged to the perimeter of the balloon. The position of the winch on a flat, nonrotating earth is considered to be the origin of an inertial two-dimensional coordinate system. The first equation expresses the motion of the balloon about its hinge point; the second expresses the motion of any link about its lower connection point.

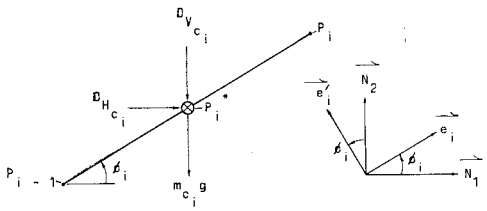

Fig. 3 Typical link.

Lagrange's differential equations of motion[3] for the system are

$$(d/dt)(\partial T/\partial \dot{\theta}) - \partial T/\partial \theta = F_\theta \tag{1}$$

and

$$(d/dt)(\partial T/\partial \dot{\phi}_r) - \partial T/\partial \phi_r = F_{\phi_r} \tag{2}$$

Cable Representation

The tether (Fig. 2) is represented by N straight links, each of identical length and connected by hinges. However, the length as well as the mass of each link is assumed to be a function of winching rate and cable mass profile. Each link is considered rigid, and each hinge, frictionless (no moments are transferred through a hinge point).

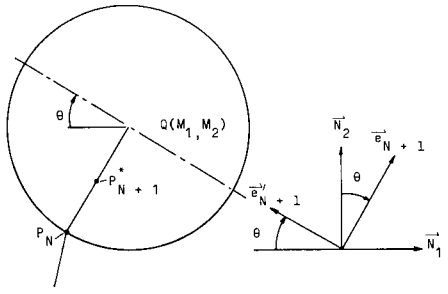

Fig. 4 Balloon and harness.

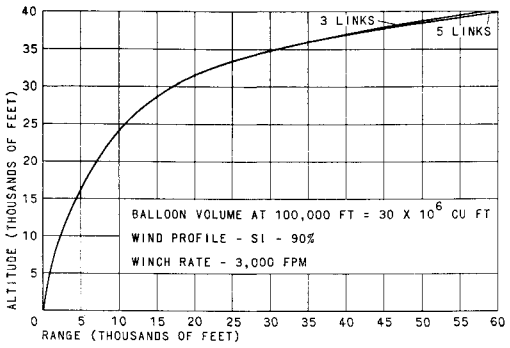

Fig. 5 Altitude vs balloon range for three- and five-link tethers.

The angle that each link makes with the horizontal (measured positive for counterclockwise rotation) is ϕ_i. All external forces on each link are assumed to be acting at the geometric center of that link.

Figure 3 shows a typical link. P_i^* is assumed to be a distance of $l_{ci}/2$ from the hinge point P_{i-1}. The velocity of P_n^* is

$$\mathbf{V}^{Pn*} = \sum_{i=1}^{n-1} l_{ci}\dot{\phi}_i \mathbf{e}_i + \sum_{i=1}^{n-1} \dot{l}_{ci}\mathbf{e}_i + \frac{l_{cn}}{2}\dot{\phi}_n \mathbf{e}'_n + \frac{\dot{l}_{cn}}{2}\mathbf{e}_n \tag{3}$$

The velocity of P_n is

$$\mathbf{V}^{Pn} = \sum_{i=1}^{n} l_{ci}\dot{\phi}_i \mathbf{e}'_i + \sum_{i=1}^{n} \dot{l}_{ci}\mathbf{e}_i \tag{4}$$

The kinetic energy of the cable follows as

$$T_c = \sum_{n=1}^{N} \left[\frac{1}{2} m_{cn} (\mathbf{V}^{Pn*})^2 + \frac{1}{2}\left(\frac{m_{cn} l_{cn}^2}{12}\right)\dot{\phi}_n^2 \right] \tag{5}$$

Balloon and Harness Representation

The balloon harness (radius of balloon) is considered to be normal to the balloon's longitudinal axis. The balloon has "directional masses" M_1 and M_2 concentrated at the center of mass of the balloon.

The balloon is assumed to be a thin, spherical, expanding shell. Consequently, the directional masses are equal and are assumed to act at the geometric center of the sphere as shown in Fig. 4. It is further assumed that pressure and temperature gradients across the balloon are zero. This eliminates phenomenon such as solar heating and thermal drag. With these two assumptions, it can be shown that the volume ratio at any altitude is equal to the inverse of the atmospheric density ratio. It follows from Eq. (4) that

$$\mathbf{V}^{P_{N+1}*} = \sum_{i=1}^{N} l_{ci}\dot{\phi}_i \mathbf{e}'_i + \sum_{i=1}^{N} \dot{l}_{ci}\mathbf{e}_i - \frac{1}{2} l_h \dot{\theta}\mathbf{e}'_{N+1} \tag{6}$$

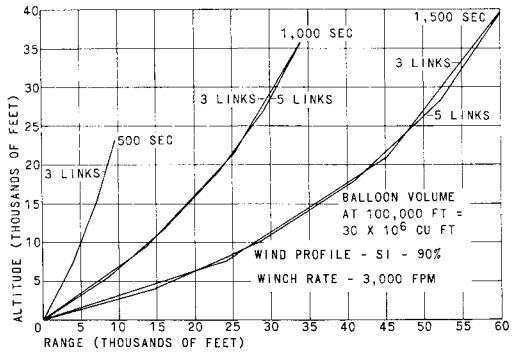

Fig. 6 Three- and five-link tether profiles.

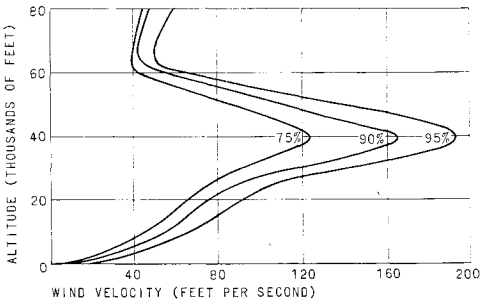

Fig. 7 Summer I wind profiles.

and

$$\mathbf{V}^Q = \sum_{i=1}^{N} l_{c_i}\dot{\phi}_i \mathbf{e}'_i + \sum_{i=1}^{N} \dot{l}_{c_i}\mathbf{e}_i - l_h\dot{\theta}\mathbf{e}'_{N+1} \tag{7}$$

The value of $\dot{l}_h$ is small when compared to $\dot{l}_c$ and is therefore ignored. The kinetic energy of the harness plus the balloon is

$$T_b = \frac{1}{2}\left(\frac{m_h l_h^2}{12}\right)\dot{\theta}^2 + \frac{m_h}{2}(\mathbf{V}^{P_{N-1}*})^2 + \frac{M_1}{2}(\mathbf{V}^Q\cdot\mathbf{e}_{N+1})^2 + \frac{M_2}{2}(\mathbf{V}^Q\cdot\mathbf{e}'_{N+1})^2 + \frac{I_B}{2}\dot{\theta}^2 \tag{8}$$

Inertial Terms

The total kinetic energy of the system is the sum of Eqs. (5) and (8):

$$T = \sum_{n=1}^{N}\left[\frac{1}{2}m_{c_n}(\mathbf{V}^{P_n*})^2 + \frac{1}{2}\left(\frac{m_{c_n}l_{c_n}^2}{12}\right)\dot{\phi}_n^2\right] + \frac{1}{2}\left(\frac{m_h l_h^2}{12}\right)\dot{\theta}^2 + \frac{m_h}{2}(\mathbf{V}^{P_{N+1}*})^2 + \frac{M_1}{2}(\mathbf{V}^Q\cdot\mathbf{e}_{N+1})^2 + \frac{M_2}{2}(\mathbf{V}^Q\cdot\mathbf{e}'_{N+1})^2 + \frac{I_B}{2}\dot{\theta}^2 \tag{9}$$

When Eq. (9) is substituted into Eqs. (1) and (2), the differential equations of motion are obtained. These equations are presented in Ref. 4.

Generalized Forces[3]

The external torque acting on the balloon (F_θ) may be determined by the following equation:

$$F_\theta = \mathbf{F}_{N+1}\cdot\frac{\partial\mathbf{V}^{P_{N+1}*}}{\partial\dot{\theta}} + \mathbf{F}_Q\cdot\frac{\partial\mathbf{V}^Q}{\partial\dot{\theta}} + \sum_{i=1}^{N}\mathbf{F}_i\cdot\frac{\partial\mathbf{V}^{P_i*}}{\partial\dot{\theta}} + M \tag{10}$$

Simplification of Eq. (10) yields

$$F_\theta = l_h(H\cos\theta - B\sin\theta) \tag{11}$$

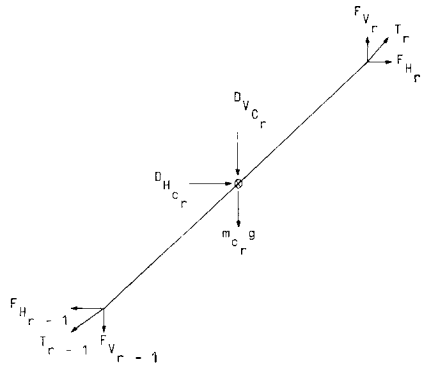

Fig. 8 Forces acting on the rth link.

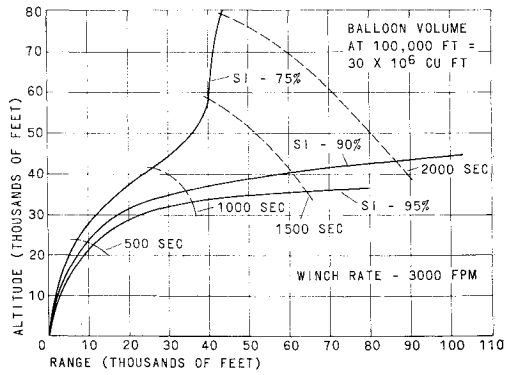

Fig. 9 Effect of wind profile on balloon launch trajectory.

The external torque acting on the rth link is given by

$$F_{\phi_r} = \mathbf{F}_{N+1}\cdot\frac{\partial\mathbf{V}^{P_{N+1}*}}{\partial\dot{\phi}_r} + \mathbf{F}_Q\cdot\frac{\partial\mathbf{V}^Q}{\partial\dot{\phi}_r} + \sum_{i=1}^{N}\mathbf{F}_i\cdot\frac{\partial\mathbf{V}^{P_i*}}{\partial\dot{\phi}_r} \tag{12}$$

Simplification of Eq. (12) yields

$$F_{\phi_r} = -\frac{l_c}{2}D_{H_{c_r}}\sin^2(\phi_r) - \frac{l_c}{2}D_{V_{c_r}}\cos^2(\phi_r) - m_{c_r}g\frac{l_c}{2}\cos(\phi_r) + l_c\sum_{i=r+1}^{N}[-D_{H_{c_i}}\sin^2(\phi_i)\cos(\phi_r-\phi_i) - D_{V_{c_i}}\cos^2(\phi_i)\cos(\phi_r-\phi_i) - m_{c_i}g\cos(\phi_r)] + l_c[-H\sin(\phi_r) + B\cos(\phi_r)] \tag{13}$$

Numerical Integration Technique

The $N+1$ equations of motion that must be solved can be written in the following form:

$$\ddot{\theta} = f(\dot{\theta},\theta,\ddot{\phi}_1\ldots\ddot{\phi}_N,\dot{\phi}_1\ldots\dot{\phi}_N,\phi_1\ldots\phi_N,t)$$
$$\ddot{\phi}_r = g(\ddot{\theta},\dot{\theta},\theta,\phi_1\ldots\ddot{\phi}_{r-1},\ddot{\phi}_{r+1}\ldots\ddot{\phi}_N,\dot{\phi}_1\ldots\dot{\phi}_N,\phi_1\ldots\phi_N,t) \tag{14}$$

Equations (14) are solved by Runge-Kutta (fourth-order accuracy) numerical integration techniques.

Because of the long real times involved in a deployment or retrieval, it is advantageous to use a large time increment in the numerical integration. Since an increase in the degrees of freedom requires a reduction in the time increment, the balloon's pitch angle is held constant, thereby eliminating the θ equation. As might be expected of a spherical balloon, computer runs show that the pitch dynamics of the balloon have negligible effect on the dynamics of the system.

To determine the number of links necessary to present a good simulation, a three-link tether is compared to a five-link tether in Figs. 5 and 6. Figure 5 shows an altitude vs range trajectory of the balloon for both three links and five links. Figure 6 shows tether profiles at 500, 1000, and 1500

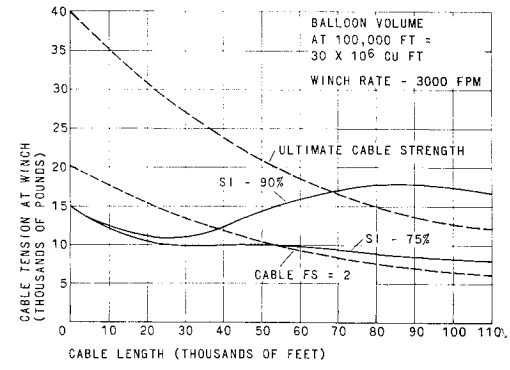

Fig. 10 Effect of wind profile on cable tension at winch.

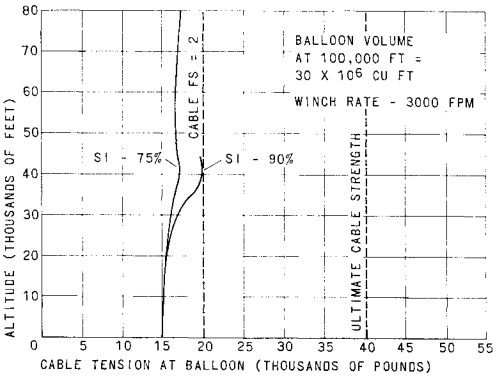

Fig. 11 Effect of wind profile on cable tension at balloon.

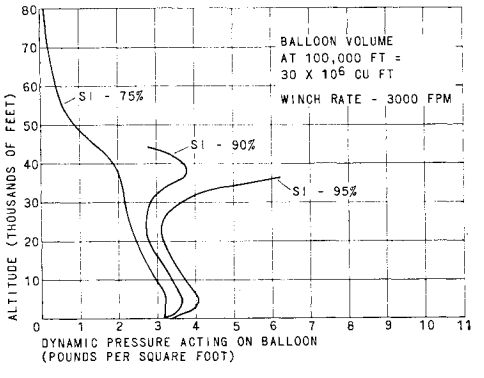

Fig. 12 Effect of wind profile on dynamic pressure acting on balloon.

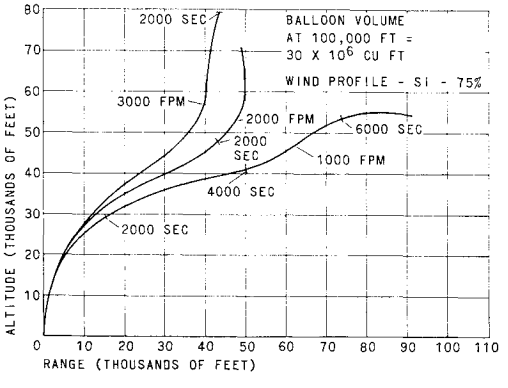

Fig. 13 Effect of winching rate on balloon launch trajectory.

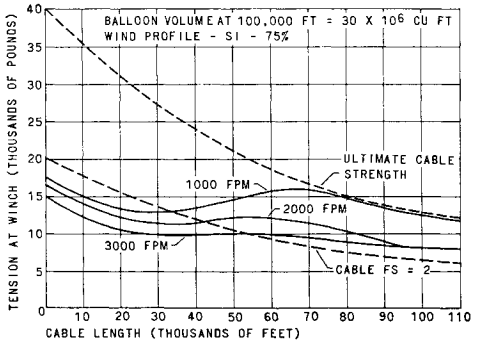

Fig. 14 Effect of winching rate on cable tension at winch.

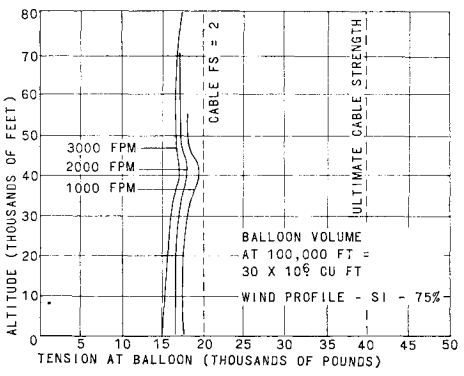

Fig. 15 Effect of winching rate on cable tension at balloon.

sec after launch for three links and five links. These comparisons justify the use of three links for an adequate simulation, a conclusion also reached by Elnan and Evert.[2]

Dynamic Pressure

For structural design purposes, the dynamic pressure on the balloon is calculated as

$$q_B = (\rho/2)[(\dot{X} - V_g)^2 + \dot{Z}^2] \tag{15}$$

For this study, three wind profiles were defined as Summer I, 75 percentile, 90 percentile, and 95 percentile. A 75-percentile wind of V fps assumes that the wind velocity is less than or equal to V fps 75% of the time. Summer I wind profiles are presented in Fig. 7.

Tension in Tether

To show how much loading the tether must be able to accommodate, the tension at each hinge point is found by summing vertical and horizontal forces acting on each link. Figure 8 shows the horizontal and vertical forces acting on the rth link.

In general, the tension at the bottom of the rth link is

$$T_{r-1} = [(F_{V_{r-1}})^2 + (F_{H_{r-1}})^2]^{1/2} \tag{16}$$

The tension at the top of the Nth link is found by summing forces acting on the balloon.

Results of Ascent and Descent Feasibility Study

The results of a limited number of computer runs are presented to show the capabilities of the computer program in a feasibility study. The basic criterion of the balloon-tether system is that the balloon support a cable in equilibrium at 100,000 ft in a 75-percentile wind.

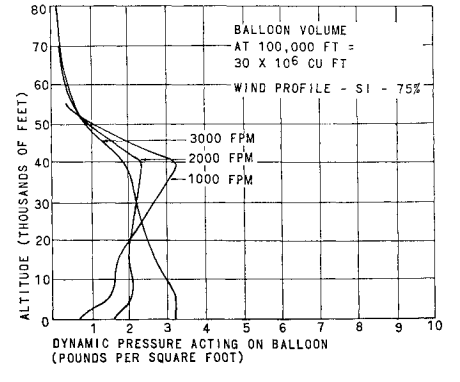

Fig. 16 Effect of winching rate on dynamic pressure acting on balloon.

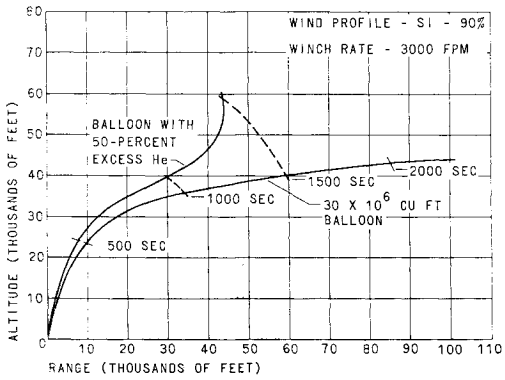

Fig. 17 Effect of excess buoyancy on balloon launch trajectory.

The cable is a Glastran tapered tether designed to support twice the tension encountered during the aforementioned equilibrium condition. The purpose of this study is to determine whether or not this system (defined by static conditions) can satisfy the dynamic conditions of ascent and descent. In the study, effects of wind profile, winching rate, and buoyant lift are established.

Figures 9–12 compare the effects of three different Summer I wind profiles. As may be seen in Fig. 9, the 30,000,000-ft^3 balloon lacks the buoyant lift to pull it through the high dynamic pressure region of a 90- or 95-percentile wind. However, the same balloon will ascend in a 75-percentile wind.

Figure 10 demonstrates that a balloon of this size will break its tether at the winch if the launch is attempted in a 90-percentile wind. However, an ascent in a 75-percentile wind does not seriously stress the tether. Figure 11 indicates that the tether strength at the balloon is more than adequate for a launch in either a 75- or 90-percentile wind.

A graph of dynamic pressure experienced by the balloon vs altitude is presented in Fig. 12. Such information would be useful in structural design of the balloon.

Figures 13–16 display the merits of a fast winching rate. A slow winching rate tends to hold the balloon back, thereby causing it to drift excessively downrange before it transcends the high dynamic pressure region (see Fig. 13). If the winching rate is too slow, the tension at the winch may exceed its ultimate strength as shown in Fig. 14,

Figure 16 shows an interesting trend in dynamic pressure. An intermediate winching rate produces a fairly constant dynamic pressure (up to an altitude of 40,000 ft); the maximum dynamic pressure at the intermediate rate is significantly less than slower or faster winching rates.

Figures 17–20 demonstrate the effect of an excess of helium at launch in a Summer I, 90-percentile wind. The ascent of the balloon with 50 percentile excess helium (see Fig. 17) was, of course, more rapid. However, the tether and balloon were submitted to greater tensions and dynamic pressures, and the tether reached its ultimate cable strength quicker than with the normal balloon (see Figs. 18–20).

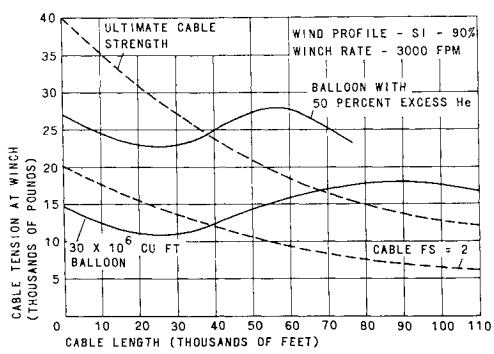

Fig. 18 Effect of excess buoyancy on cable tension at winch.

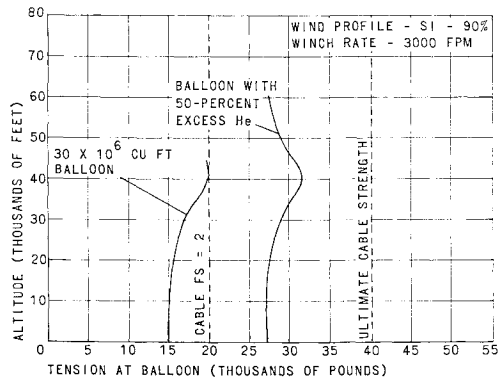

Fig. 19 Effect of excess buoyancy on cable tension at balloon.

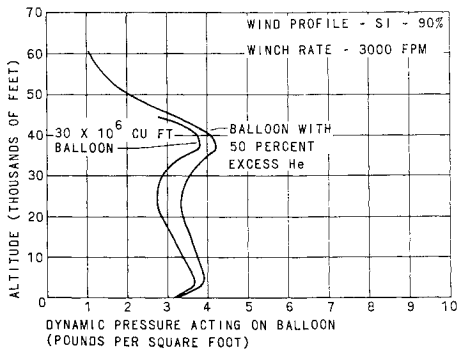

Fig. 20 Effect of excess buoyancy on dynamic pressure acting on balloon.

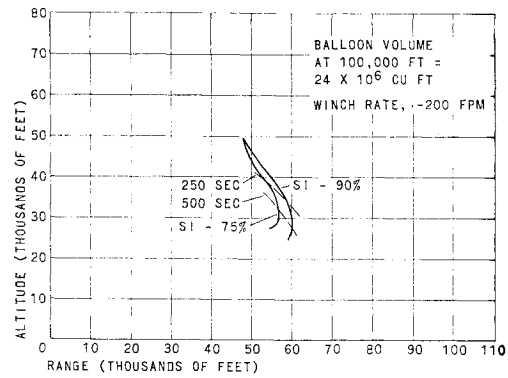

Fig. 21 Effect of wind profile on balloon retrieval trajectory.

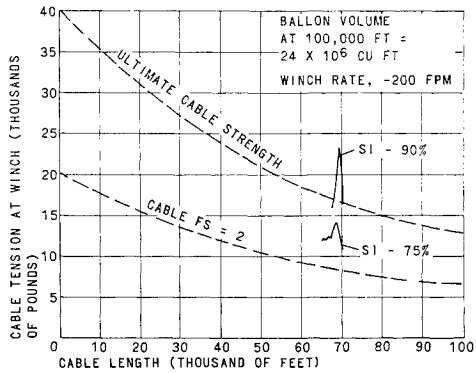

Fig. 22 Effect of wind profile on cable tension at winch.

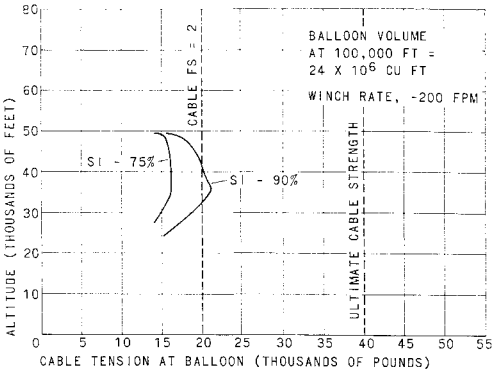

Fig. 23 Effect of wind profile on cable tension at balloon.

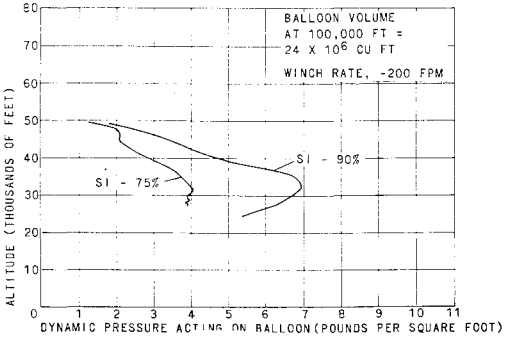

Fig. 24 Effect of wind profile on dynamic pressure acting on balloon.

To demonstrate the versatility of the computer-program simulation, Figs. 21–24 present retrieval trajectory characteristics. To stay within the ultimate cable strength, winching rates during retrieval were reduced one order of magnitude below launching rates. It was also found necessary to valve 20 percentile of the helium from the balloon to keep the buoyant force low. Figure 21 shows downwind displacement effects of Summer I, 75-and 90-percentile wind profiles. Figures 22–24 demonstrate the significant increase in tensions and dynamic pressures over launches in the same wind profiles (Figs. 10–12).

Conclusions

To keep the complexity of the equations of motion and the computer program to a minimum, several assumptions and approximations were introduced. However, the results obtained are considered sufficiently meaningful and accurate to demonstrate the feasibility of the launch and retrieval of a high-altitude balloon.

The results of the study indicate that this system can be launched and retrieved under certain conditions and establish some preliminary design criteria for the balloon, tether, and winch. A detailed derivation of the equations of motion, a complete discussion of the computer program, and further analysis of computer runs are presented in Ref. 4

References

[1] Vorachek, J. J., "High-Altitude Tethered Balloon Systems Study," GER-13790, March 1968, Goodyear Aerospace Corp., Akron, Ohio.

[2] Elnan, O. R. and Evert, C. G., "Dynamics of Tethered Balloon in the Longitudinal Plane," GER-12901, Oct. 1966, Goodyear Aerospace Corp., Akron, Ohio.

[3] Goldstein, H., *Classical Mechanics*, Addison-Wesley, Cambridge, Mass., 1950.

[4] Doyle, G. R. and Vorachek, J. J., "Mathematical Model and Computer Program for the Ascent and Descent of High-Altitude Tethered Balloons," GER-13714, Feb. 1968, Goodyear Aerospace Corp., Akron, Ohio.